Transport properties of CdS quantum dots by chemical precipitation method

D. NITHYAPRAKASH[a,b*], J. CHANDRASEKARAN[a], B. PUNITHAVENI[b]
[a]*PG and Research, Department of Physics, Sri Ramakrishna Mission Vidyalaya College of Arts and Science, Coimbatore – 641 020, Tamilnadu, India*
[b]*Department of Physics, PPG Institute of Technology, Coimbatore-641 035, Tamilnadu, India*

In the present work, chemical precipitation method was employed for the preparation of CdS quantum dots. XRD studies reveal that CdS in single phase hexagonal structure. The particle size of CdS nanoparticles is obtained as 3 nm and also confirmed through HRTEM. Morphology and elemental mapping of the synthesized nanoparticles were studied by SEM and EDX analyses. The optical properties were studied by the ultraviolet – visible absorption spectrum and photoluminescence spectroscopy. The D.C electrical measurements of CdS nanoparticles pellet were performed using two probe techniques. The A.C conductivity and dielectric properties of pellet analyzed in the frequency range 100 kHz –1 MHz indicates that the dielectric constant and loss tangent increases with increase in temperature and decrease with increase in frequency in addition it supported the hopping mechanism.

(Received April 22, 2015; accepted September 9, 2015)

Keywords: Cadmium sulfide; Quantum dots; Conductivity; Dielectric properties

1. Introduction

The semiconductor nanoparticles exhibit structural, electronic, optical, luminescence and photoconducting properties [1-6] very different from their bulk properties. II-VI semiconductor nanoparticles are currently of great interest for their practical applications such as zero-dimensional quantum confined materials in optoelectronics and photonics. Among II-VI compounds, CdS with a direct band gap, Eg=2.40 eV, is an important semiconductor with non-linear optical properties have been extensively studied and has potential applications such as solar battery, photoelectrocatalysis, Biological sensors and photodiodes [7-16]. The Bohr radius of exciton is 3 nm for CdS and the quantum confinement effect occurs when the size of crystallites is around 2 – 6 nm and below [17].

In this paper deals with the preparation of CdS nanoparticles using chemical precipitation method and characterization of the CdS nanoparticles by FTIR, XRD, SEM, HR-TEM, EDAX, UV–Vis and photoluminescence spectroscopy. Electrical conductivity was analyzed with dielectric studies using pressed pellets.

2. Experimental

Analytical grade cadmium acetate ($Cd(CH_3COO)_2$) and sodium sulfide (Na_2S) were purchased from merck and were used without further purification. Solutions of cadmium acetate and solutions of sodium sulfide (1:1 molar ratio) were taken as the precursors individually. Both the solutions were stirred continuously until dissolved well. The solution of Na_2S is added drop wise to solution of $Cd(CH_3COO)_2$ with constant stirrering. Then the solution were mixed together and stirred vigorously. After the precipitation the formed CdS was filtered and washed with methanol, ethanol and deionized water. Then the product was dried at 100 C for 3 h and grained. The powder was pressed to form pellets by using hydraulic press.

3. Characterization

FTIR analysis was carried out over a range of 400–4000 cm^{-1}using Spectrum RXI. Transmission spectra were obtained by forming a thin KBr pellet containing CdS powder. X-ray diffraction pattern for CdS nanoparticles was obtained using Shimadzu XRD-6000 with CuKα radiation (α = 1.5405Å). The UV–Vis spectrum of CdS nanoparticles was analyzed by JASCO-V570. A Photoluminescence spectrum was recorded using FP – 6500 Sspectroflurometer. CdS nanoparticles pellet applied with silver paste on both sides was sandwiched between two copper electrodes to obtain a better contact. Digimatic Micrometer has been used for the determination of the pellet thickness. The DC electrical measurements of the obtained CdS pellet was performed within the temperature range of 303–363 K using two probe technique. The A.C conduction of CdS nanoparticles was measured using computerized HIOKI LCR METER 3532-50 in the frequency range 100 kHz–1MHz at different temperature.

4. Results and Discussion

4.1 Structural properties

Figure. 1 shows the X- ray diffraction pattern of CdS nanoparticles. The pattern shows peaks at 26.60°, 43.80° and 51.90° which corresponds to the (002), (110) and (112) planes of the hexagonal phase. The broadening of diffraction peak provides information about crystallite size. As the width increases, the particle size of the crystal decreases and vice versa [18]. The diffraction pattern has broad diffraction peaks that suggest that the particles are of nanocrystalline nature. The lattice constants have been calculated using the formula

$$\frac{1}{d^2} = \frac{4}{3}\left(\frac{h^2 + hk + l^2}{a^2}\right) + \left(\frac{l^2}{c^2}\right) \quad (1)$$

where 'a' and 'c' are the lattice constants, d is the interplanar spacing. The lattice constants have been found to be a = 4.121 Å and c = 6.682 Å and they match well with the JCPDS data (80-0006).

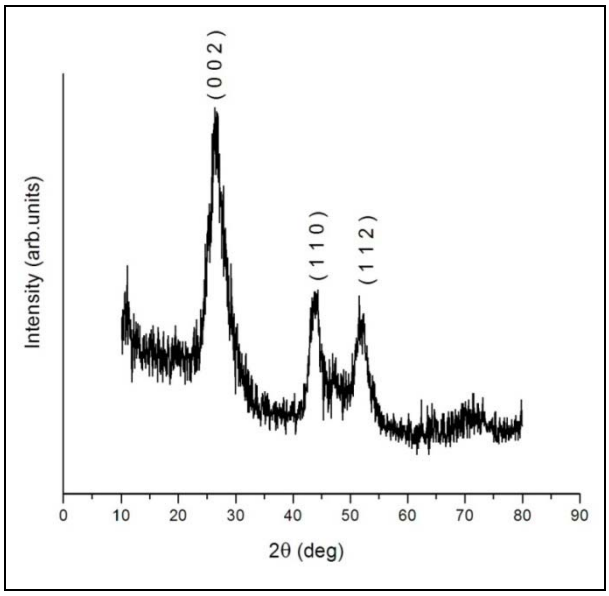

Fig.1. XRD pattern of CdS nanoparticles

The average crystallite size (D) of the CdS particles has been calculated using Scherrer's equation [19].

$$D = \frac{0.94\lambda}{\beta \cos\theta} \quad (2)$$

where λ is the wavelength of X-rays, β is the FWHM and θ is the diffraction angle. The average particle size is found to be 3 nm.

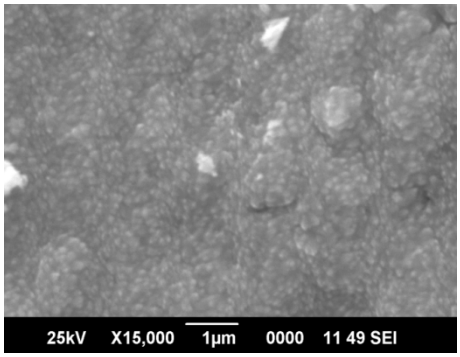

Fig.2. SEM image of CdS nanoparticles

Fig. 2 shows the SEM image of the CdS nanoparticles. The growth of the fine particles of CdS in a regular pattern is observed on the surface of the sample.

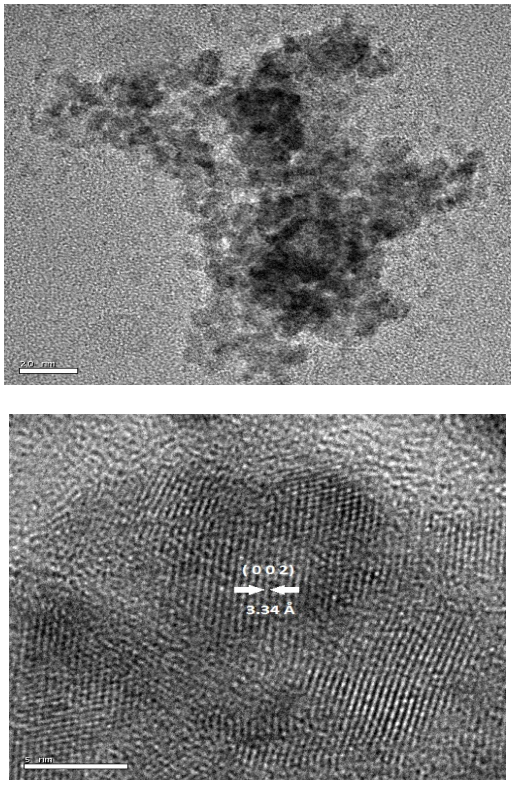

Fig. 3 HRTEM image of CdS nanoparticles.

HRTEM micrograph of CdS nanoparticles is shown in figure.3. There are no visible single particles in the HRTEM image and it is observed that the particles have got agglomerated. The particle size has been found to be around 4 nm. The image also shows the presence of lattice fringes, the inter planar spacing has been found for the lattice fringes and it is found to 3.34 Å which corresponds to (0 0 2) plane of hexagonal CdS.

The energy dispersive analysis by X – rays spectra of CdS is shown in fig. 4. The spectrum has only cadmium and sulphur peaks and it confirms that the sample is composed of cadmium and sulphur. It is evident from the peaks of the figure that the product is highly pure. The

pattern shows the presence of 44.57 at % of Cd and 55.43 at % of S.

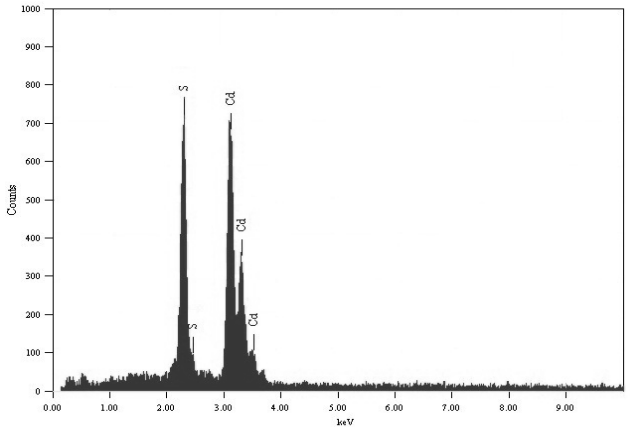

Fig.4 EDAX spectrum of CdS nanoparticles

4.2 Optical studies

Optical absorption spectra of CdS nanoparticles is shown in fig. 5. The absorption onset wavelength is 473 nm. The absorption edge of the CdS sample exhibits a strong blue shift when compared to the value of bulk CdS (512 nm) and it clearly indicates the formation of nanoparticles. The fundamental absorption which corresponds to the electron excitation from the valance band to the conduction band can be used to determine the nature and the value of the optical band gap. The relation between absorption coefficient (α) and the incident photon energy (hν) can be written as [20]

$$(\alpha h\nu)^n = A(h\nu - E_g) \quad (3)$$

where, α is optical absorption coefficient from the absorption data, hν is the photon energy, A is a constant and the exponent n depends on the type of transition. The plot of $(\alpha h\nu)^2$ versus hν of CdS nanoparticles is shown in Fig. 6. The straight-line nature of the plot reveals that the transition in CdS nanoparticles is direct-allowed. The optical band gap values of CdS nanoparticles estimated from the intercept of the straight line is shown in fig. 6. The band gap is found to be 2.97 eV. The observed direct band gap is much higher than that of the bulk value of CdS (2.42 eV) [21, 22], because of the quantum confinement. Also it is evident that for CdS like nanoparticles, the relation between mean size of the grains and the onset absorption wavelength related by Henglein's empirical formula [23]

$$2R_{CdS} = \frac{0.1}{(0.4310 - 0.0002148\lambda_e)} \quad (4)$$

where λ_e is the wavelength of absorption onset. The particle size has been calculated and is 2.2 nm. The particle size obtained from X-diffraction, HRTEM and optical absorption studies is smaller than the Bohr radius of 3 nm for CdS, the strong confinement effect can be assumed to be present in the CdS quantum dots.

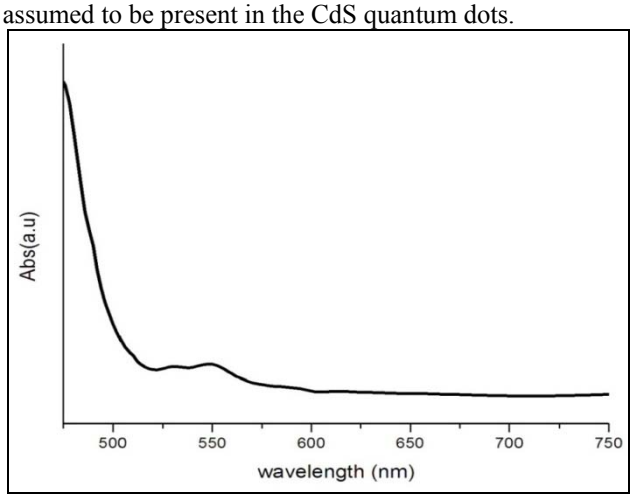

Fig.5 UV-VIS absorption spectrum of CdS nanoparticles

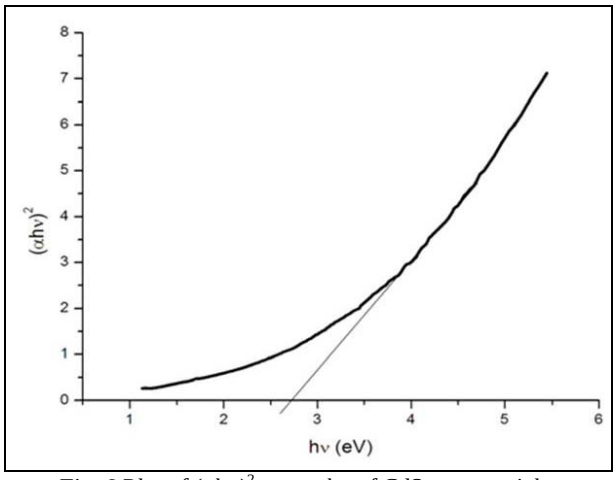

Fig. 6 Plot of $(\alpha h\nu)^2$ versus hν of CdS nanoparticles

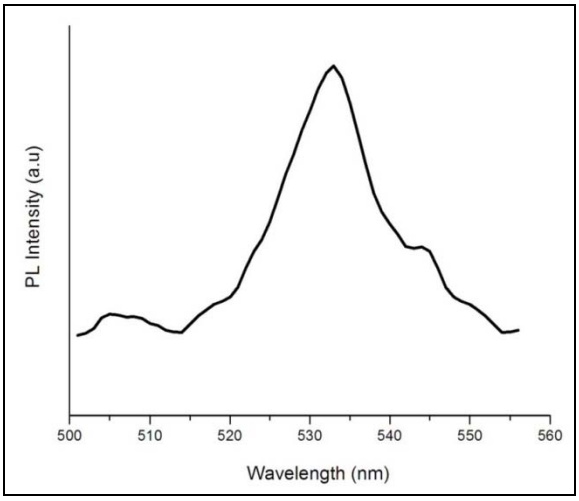

Fig. 7 The photoluminescence spectrum of CdS nanoparticles

The photoluminescence spectra of CdS nanoparticles is shown in fig. 7. The photoluminescence spectra of the CdS nanoparticles has been obtained using an excitation

wavelength of 324 nm. The spectra exhibits one strong emission peak at 533 nm that corresponds to radiative recombination of quantum confined electron–hole pair whose energy is smaller than the energy bandgap of nanoparticles. The radiative recombination of excitons is by absorption of electrons lying at higher excited energy levels [24]. The emission present at 533 nm is known as green emission band of CdS.

Using the photoluminescence spectra the band gap has been calculated using the formula

$$E_g = \frac{hc}{\lambda} \quad (5)$$

where, E_g is the band gap energy, h is Planck's constant and c is velocity of light, λ is wave length (m). The band gap (E_g) has been found to be 2.31 eV [21,22].

4.3 DC Conductivity

The I-V characteristics of CdS nanoparticles were measured at different temperatures and found to be linear in all the cases as shown in figure.8. This linearity of I-V characteristics is an ohmic nature (I α V), indicating that the current is controlled by generated carriers. This is Ohmic behavior that was understood on the basis that at the low voltages there is no injection of carriers from the electrode contact and the initial current is governed by the intrinsic free-carrier motion. In our samples, CdS semiconductor nanoparticles have a small energy bandgap and small amount of energy is sufficient to excite electrons from full valence band to conduction band. From the I – V characteristics of the sample, the value of electrical conductivity has been obtained using the formula

$$\sigma = \frac{IL}{VA} \quad (6)$$

where I is the current, V is the voltage, L is the thickness and A is the area of cross section of the sample. The D.C conductivity obtained at room temperature was 1.458×10^{-6} S/cm.

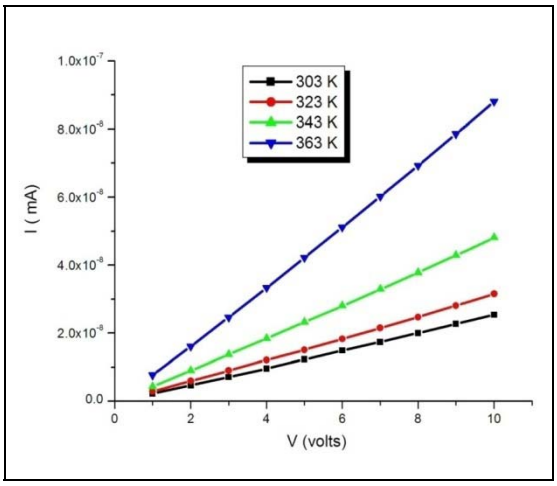

Fig. 8 I – V characteristics of CdS

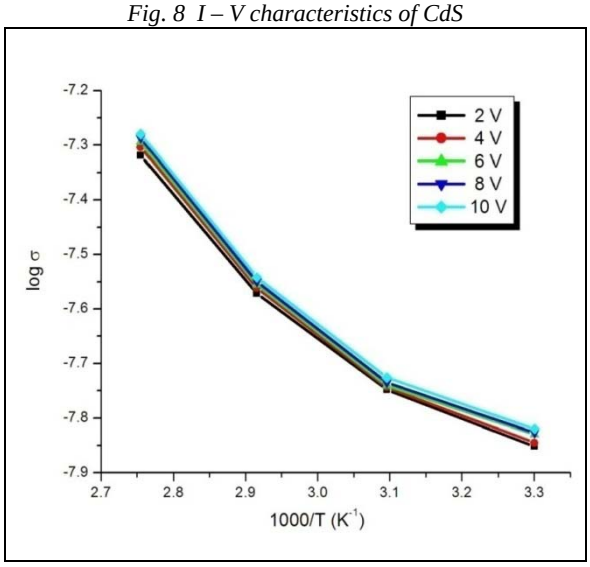

Fig.9 Plot of logarithm of conductivity versus inverse temperature of CdS

The plot of 1000/T versus log σ is shown in figure. 9. The electrical conductivity is observed to vary with temperature according to the Arrhenius equation [25]

$$\sigma = \sigma_0 \exp\left(\frac{-E_a}{kT}\right) \quad (7)$$

where σ_0 is a constant, E_a is the activation energy, k is the Boltzmann constant and T is the absolute temperature.

The slope of these plots given the value of activation energies. The activation energy is 92.98 meV .

4.4 A.C Conductivity and Dielectric Properties of CdS

The dielectric constant and dielectric loss of the CdS nanoparticles have been measured in the frequency range of 100 kHz – 1 MHz at different temperatures. The dielectric constant of CdS was calculated from the following equation

$$\varepsilon' = \frac{Cd}{\varepsilon_0 A} \quad (8)$$

where d is the thickness of the sample, A is the area of the sample. ε_0 is the permittivity of free space. The dielectric constant was measured as a function of the frequency at different temperatures and is shown in figure.10. It is observed that the dielectric constant decreases exponentially with increasing frequency and then attains almost a constant value in the high frequency region. It is also observed that the dielectric constant increases with increase in the temperature. The high value of the dielectric constant at low frequencies may be due to the presence of all the four polarizations namely, space charge, orientation, electronic and ionic polarization and its low value at higher frequencies may be due to the gradual loss of significance of these polarizations [26].

This may lead to large values of dielectric constant at low frequencies.

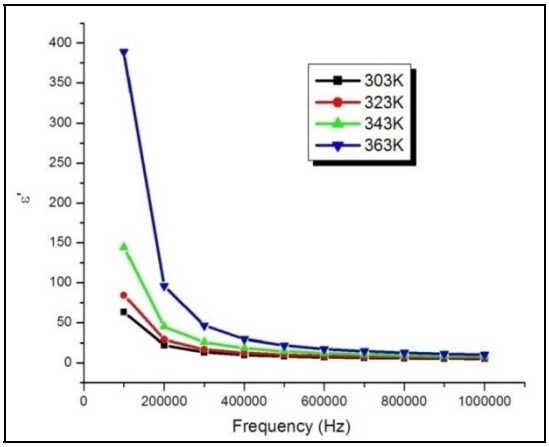

Fig. 10 Variation of dielectric constant with frequency for CdS

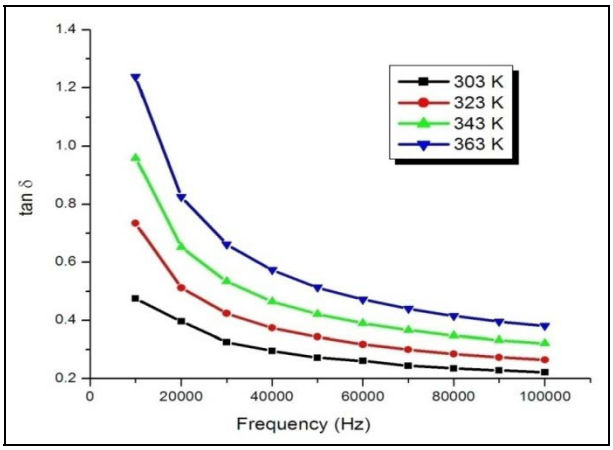

Fig. 11 Variation of dielectric loss with frequency for CdS

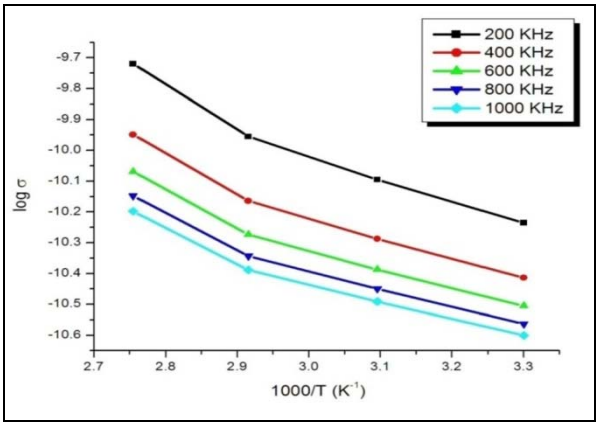

Fig. 12 Variation of log conductance with inverse absolute temperature for CdS

The dielectric loss has been studied as a function of frequency at different temperatures and is shown in figure.11. The curves suggest that the dielectric loss is strongly dependent on the frequency of the applied field, similar to that of the dielectric constant.

The dielectric loss decreases with an increase in the frequency at all the studied temperatures, but appears to achieve a constant value in the higher frequency range of 1 MHz and above. In the low frequency region, high energy loss is observed, which may be due to the dielectric polarization, space charge and orientation polarization occurring in the low frequency range.

The temperature dependence of the AC conductivity at different frequencies was studied for the CdS nanoparticles. Fig.12 shows the plot of log σ against 1000/T for the CdS nanoparticles. It is clear from the figure that log σ decreases with the reciprocal of absolute temperature. This suggested that the AC conductivity is a thermally activated process arising from the different localized states in the band gap or in its tails. The activation energy (ΔE) of conduction is calculated at different frequencies using the equation,

$$\sigma = \sigma_0 \exp\left(\frac{-E_a}{k_B T}\right) \quad (9)$$

where, σ_0 is a constant.

It is observed that the conductivity increases with increase in temperature. The activation energies are estimated as 114 and 102 meV for the frequencies 200 Hz and 1 kHz, respectively. The activation energy is seen to decrease with the increase in frequency. Thus as frequency increase the activation energy decreases and this characteristic of thermally activated hopping.

5. Conclusion

CdS quantum dots have been successfully prepared using a simple chemical solution method. EDAX analysis confirmed the purity of the sample. X-ray diffraction analysis confirms the formation of hexagonal structure of CdS with average grain size of 3 nm. Optical absorption property of CdS showed a blue shift in their absorption band edge and it is explained due to the quantum size effect of the CdS nanoparticle. The photoluminescence spectra of CdS exhibited broad green emission band centered at around 533 nm. The D.C. electrical conductivity of the CdS has been analyzed in the temperature range from 303–363 K. Activation energy of the carrier obtained was found to be in the order of millielectronvolt. The A.C. conductivity, capacitance, dielectric constant and dielectric loss of the CdS depends frequency and temperature. The activation energy in A.C. conduction was suggested to be hopping mechanism. Thus, the present method is a simple and efficient for the preparation of nano-crystalline CdS nanoparticles at low temperature with excellent structural and optical properties which could find their applications in optoelectronic devices.

References

[1] A. Palivisatos, Science **271**, 933 (1996).
[2] X. G. Peng, L. Manna, W. D. Yang, J. Wickham, E. Scher, A. Kadavanich , A. P Alivisatos, Nature (London) **404**, 59 (2000).
[3] M. G. Bawendi, M. L. Steigerwald , L. E .Brus, Annu. Rev. Phys. Chem. **41**, 477 (1990).
[4] T.Trindade, P .O'Brien, N. L.Pickett, Chem. Mater. **13**, 3843 (2001).
[5] M. G. Bawendi, P. J. Caroll, W. L. Wilson, L. E Brus, J. Chem. Phys. **96**, 1335 (1992).
[6] V. L. Colvin, M. C. Schlamp, A. P Alivisatos, Nature (London) **370**, 354 (1994).
[7] R. Rossetti, S. Nakahara, L.E. Brus, J. Chem. Phys. **79**, 1086 (1983).
[8] A. Berman, D. Charych, Adv. Mater. **11,** 296 (1999).
[9] C. J. Barrelet, Y. Wu, C.M. Lieber, J. Am. Chem.Soc. **125,** 11498 (2003).
[10] D. L. Klein, R. Roth, A. K. L. Lim, A. P. Alivisatos, Nature **389**, 699 (1997).
[11] A. Mews, A. Eychmullar, M. Giersig, D. Shoos, J. Weller, J. Phys. Chem. **98**, 934 (1994).
[12] C. T. Tsai, D. S. Chouu, S. L. Yang, J. Appl. Phys. **79**, 9105 (1996).
[13] N. Tessler, V. Medvedev, M. Kazes, U. Banin, Science **295**, 1506 (2002).
[14] H.Mattoussi, L. H. Radzilowski, B. O. Dabbousi, E. L. Thomus, M. G. Bawendi, M. F. Rubner, J. Appl. Phys. **83**, 7965 (1998).
[15] T. Taguchi, Y. Endoh, Y. Nozue, Appl. Phys. Lett. **56**, 342 (1991).
[16] S. H. Sun, C. B. Murray, J. Appl. Phys. **85**, 4325 (1999).
[17] S.M. Reda, Acta Mater **56**, 259 (2008).
[18] B.D.Cullity, S.R.Stock, Elements of X-ray diffraction, Prentice Hall, New Jersey, (2001), Chapter 14.
[19] J.G. Deng, X.B. Ding, W.C. Zhang, Y.X. Peng, J.H. Wang, X.P. Long, P.Li, S.C. Chen, Polymer **43**, 2179 (2002).
[20] J.I. Pankove, Optical Processes in Semiconductors, Prentice Hall, Englewood Cliffs, NJ, (1971).
[21] R. Banerjee, R. Jayakrishnan, P. Ayyub, J. Phys. Condens. Matter, **12**, 10647 (2000).
[22] Der San Chuu, Chang Ming Dai, Phys. Rev. B **45**, 11805 (1992).
[23] L. Spanhel, M. Haase, H. Weller, A. Henglein, J. Am. Chem. Soc. **109**, 5649 (1987).
[24] S.V. Gaponendo, Optical properties of semiconductors nano-crystals, Cambridge University Press, Cambridge. (1998), doi:10.2277/0521582415.
[25] M. Gosh, A. Barman, A.K. Meikap, S.K. De, S. Chatterjee, Phys. Lett. A **260**, 138 (1999).
[26] C.P. Smyth, Dielectric Behavior and Structure, McGraw-Hill, New York, (1965) p. 132.

*Corresponding author: nithip12@gmail.com